

Adsorption of Methyl Hydroperoxide (CH₃OOH) on Water Ice. Theoretical Study with Systematic Assessment of Coordination Modes

Stanislav K. Ignatov,^{*,†,‡} Oleg B. Gadzhiev,[‡] Mikhail Yu. Kulikov,[§] Alexander I. Petrov,[⊥] Alexey G. Razuvaev,[‡] Michael Gand,[†] Alexander M. Feigin,[§] and Otto Schrems[†]

[†]Alfred Wegener Institute for Polar and Marine Research, Postfach 120161, D-27515 Bremerhaven, Germany

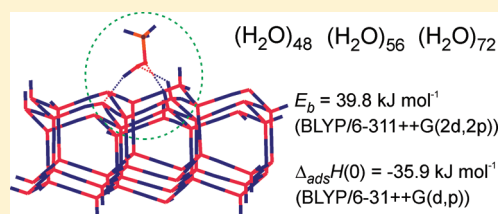
[‡]N.I. Lobachevsky State University of Nizhny Novgorod, 23 Gagarin Avenue, Nizhny Novgorod 603950, Russia

[§]Institute of Applied Physics of RAS, Nizhny Novgorod, 46 Ulyanova st, Nizhny Novgorod 603000, Russia

[⊥]Siberian Federal University, 81 Svobodnyi prosp., Krasnoyarsk 660041, Russia

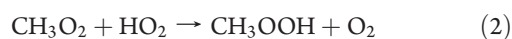
S Supporting Information

ABSTRACT: The low-temperature interaction between methyl hydroperoxide CH₃OOH (MHP) and the hexagonal water ice surface was studied using DFT (BLYP/6-31++G(d,p)) calculations. The structures, energies, and some thermodynamic properties of the molecular complexes between MHP and the water clusters (H₂O)₄₈, (H₂O)₅₆, (H₂O)₇₂ representing the surface fragments of the (0001), (10 $\bar{1}$ 0), and (11 $\bar{2}$ 0) crystallographic planes of the hexagonal oxygen lattice of the water ice Ih with proton ordering corresponding to Pisani's P-ordered model were calculated. The various modes of coordination and intrusion were studied using the extended set (up to 192 points for each plane) of the structures optimized at the semiempirical (PM3) level. The validity of the surface models was verified by the stability of the results obtained in the cluster series (H₂O)_n (n = 48, 72, 192, 216) at the semiempirical level as well as by DFT calculations of selected structures at the BLYP/6-311++G(2d,2p) level.



INTRODUCTION

Adsorption of atmospheric trace gases on microcrystalline water ice particles in the upper layers of the Earth's atmosphere are considered today as one of the most important processes of atmospheric chemistry providing the occurrence of many key reactions that are impossible under the purely gas-phase conditions.^{1,2} Such processes are, for example, the accumulation of atmospheric trace gases on ice particles of cirrus clouds in the upper troposphere and heterogeneous reactions on the surfaces of polar stratospheric cloud (PSC) particles in the stratosphere. Furthermore, interactions of atmospheric trace gases with surfaces of the ice shields in polar regions play a crucial role in tropospheric chemistry both in the Arctic and in Antarctica.³ The primary steps of this accumulation are adsorption/desorption processes. In this respect, oxidants such as hydrogen peroxide H₂O₂ and methyl hydroperoxide CH₃OOH (MHP) are very interesting because they can undergo further reactions in the ice.⁴ In polar regions, H₂O₂ and CH₃OOH are the only detectable hydroperoxides both in tropospheric air or snow and ice and hence have received special attention.⁵ Methyl hydroperoxide is the most dominant species of organic peroxides over the ocean waters and is washed out of the troposphere by rain or snow fall. MHP is mainly produced in the atmosphere by the oxidation of CH₄ according to eqs 1 and 2.



Whereas the adsorption of the H₂O₂ on the ice surface is described in detail,⁶ the interaction of the MHP molecule with the ice surface, however, has so far only been scarcely studied.⁷ Moreover, among the complexes formed by MHP, only several representatives are considered. From experimental study,⁸ it follows that the water solubility of MHP is not high in comparison with H₂O₂ (the corresponding Henry's constant of MHP is approximately 200 times lower than for H₂O₂). Thus, during the MHP interaction with the surface of ice particles, the adsorption modes of MHP should prevail over the solubility. The corresponding value for standard enthalpy of solution $\Delta H^0(298)$ obtained in ref 8 was $-43.6 \text{ kJ mol}^{-1}$, close to $-44.2 \text{ kJ mol}^{-1}$ obtained in earlier studies of Lind and Kok.^{9,10} The MHP dimer was studied by Alkorta and Elguero,¹¹ Du et al.,¹² and by Kulkarni et al.¹³ with emphasis on the chirality of the complex structures. It was shown that the BSSE-corrected binding energy at the MP2/6-311++G-(2d,2p) level was 38.6 kJ mol^{-1} (BSSE + ZPE-corrected value 31.5 kJ mol^{-1}).¹³ The MHP–H₂O₂ complex was described by Du and Zhou.¹⁴ The most favorable geometry of the complex was found to be a five-membered H-bonded ring structure with dangling CH₃ and peroxide HO fragments with a binding energy of 38.8 kJ mol^{-1} at the MP2/6-31++G(2d,2p) level (BSSE + ZPE corrected value 22.7 kJ mol^{-1}).¹⁴ The most detailed study on the interaction of MHP with water clusters was performed

Received: December 22, 2010

Revised: March 24, 2011

Published: April 20, 2011

most recently by Kulkarni et al.¹⁵ In their investigation, the structures of MHP complexes with unconstrained water clusters $(\text{H}_2\text{O})_n$ ($n = 1-5$) were studied at MP2/6-31G(d,p) and MP2/6-311++G(2d,2p) levels and the molecular interactions were thoroughly analyzed with emphasis on the role of microsolvation in the MHP oxidation reactions in the liquid phase. It was found that the binding energy of the binary complex $\text{MHP} \cdot \text{H}_2\text{O}$ at the MP2/6-311++G(2d,2p) level is 32.3 kJ mol^{-1} . The total BSSE-corrected binding energy of the largest considered cluster $\text{MHP} \cdot (\text{H}_2\text{O})_5$ is $173.7 \text{ kJ mol}^{-1}$ (ZPE-corrected value $159.0 \text{ kJ mol}^{-1}$), which gives 29.0 (26.5) kJ mol^{-1} per molecule. In all of the optimized clusters, the MHP molecule was located at the cluster surface keeping its hydrophobic CH_3 fragment dangling outside.

There are so far no experimental data on the $\text{MHP}-\text{H}_2\text{O}$ complexes available although hydroxymethyl hydroperoxide has been studied by photodissociation spectroscopy.¹⁶ However, theoretically estimated IR spectra of $\text{MHP}-\text{H}_2\text{O}$ complexes and clusters have been reported.¹³⁻¹⁵

In connection to the $\text{MHP}-\text{ice}$ interaction, it is worthwhile to mention the studies on the effects of the molecular environment on the MHP reactivity in the gas and condensed phases.^{17,18} In ref 17, the aqueous phase photooxidation of ammonia with H_2O_2 and MHP was studied under simulated droplet conditions and it was shown that the kinetic photochemical yield was sensitive to the pH value. Urakawa et al.¹⁸ have shown that the water-MHP coordination on the metal center is important in the catalytic reactions of epoxidation of olefins.

In our investigation, we studied the interaction of the MHP molecule with the ice surfaces considering extended cluster models of ice with emphasis on the structures and energies of the adsorption complexes formed on the ice surface and after intrusion of the deposited MHP molecule into the ice crystal. The main goals of our study were to obtain the data regarding the adsorption ability of atmospheric ice particles for MHP molecules and to estimate the possibility for MHP molecules to participate in further chemical and photochemical reactions at the gas-ice surface interface. Special attention has been paid to the question of how the different coordination modes contribute to the adsorption energy and to the use of proper models for the ice surface reliable enough to obtain results that are independent from the model size. For this purpose, we used the extensive preliminary exploration of the adsorption sites feasible on different crystallographic planes to select the coordination sites preferable from the energetic point of view. The selected set of the structures found in this preliminary search was used further to calculate the adsorption parameters on the higher theory level.

In addition to its high relevance for troposphere - ice (snow) surface chemistry, the system of interest has also been considered close to middle atmospheric conditions: $T = 180-220 \text{ K}$, the low pressure of air and extremely low concentrations of the adsorbed molecules. Under these conditions, the structure of the water ice mostly corresponds to the crystalline hexagonal phase (*Ih*) with a well-defined surface and the deposition of MHP can be considered as a single-molecule adsorption.

SURFACE MODELS AND THEORETICAL METHODS

The MHP adsorption on ice crystals has been modeled within the molecular cluster approximation. For this purpose, a series of clusters $(\text{H}_2\text{O})_n$ ($n = 26, 48, 56, 72, 108, 192, 216$) with the hexagonal ice-like oxygen lattice structure has been constructed as models of the ice surface. The structure of clusters was chosen

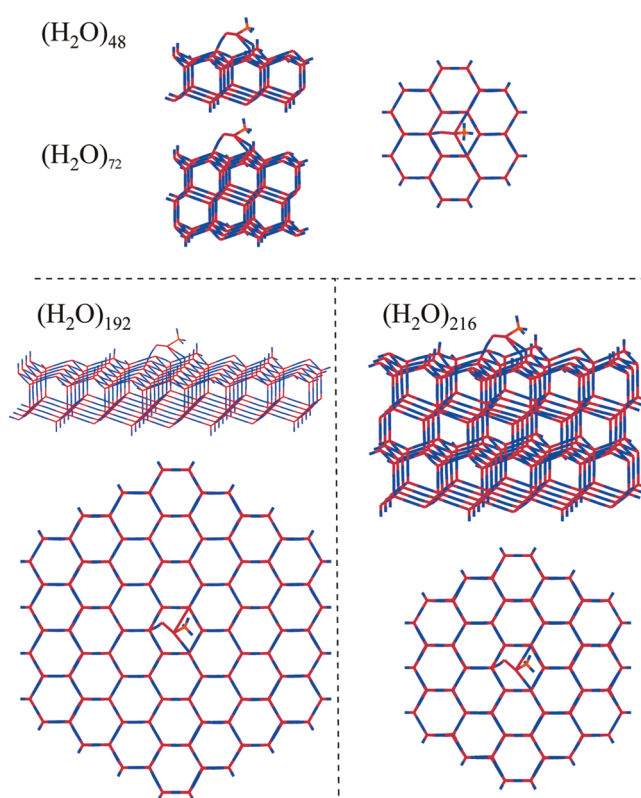


Figure 1. Selected ice clusters (with selected PM3-optimized positions of adsorbed MHP molecule) used to assess the crystal environment effects.

in such a manner to describe different sites of the ideal ice *Ih* crystal. The clusters $(\text{H}_2\text{O})_{26}$, $(\text{H}_2\text{O})_{48}$, $(\text{H}_2\text{O})_{72}$, $(\text{H}_2\text{O})_{192}$, and $(\text{H}_2\text{O})_{216}^{(0)}$ describe the (0001) (basal) plane of the hexagonal ice. The clusters $(\text{H}_2\text{O})_{56}^{(1)}$, $(\text{H}_2\text{O})_{108}$, and $(\text{H}_2\text{O})_{216}^{(1)}$ allow the modeling of the surfaces corresponding to the $(10\bar{1}0)$ plane, and the clusters $(\text{H}_2\text{O})_{56}^{(2)}$, $(\text{H}_2\text{O})_{108}$, and $(\text{H}_2\text{O})_{216}^{(2)}$ are the models of the $(11\bar{2}0)$ surface fragments. The superscripts at the cluster formula allow us to distinguish the different models with the same molecular composition. These models, for example $(\text{H}_2\text{O})_{56}^{(1)}$ and $(\text{H}_2\text{O})_{56}^{(2)}$, are distinguished not only by orientation but also by the number of boundary atoms that were fixed during the geometry optimization. Because of the large cluster size, we can show in figures only the most important structures. Hence, Figure 1 shows the clusters $(\text{H}_2\text{O})_{48}$, $(\text{H}_2\text{O})_{72}$, $(\text{H}_2\text{O})_{192}$, $(\text{H}_2\text{O})_{216}$ demonstrating the series of structures of extending size used below to assess the crystal environment effects.

The preliminary calculations performed on both DFT and PM3 levels show that the cluster $(\text{H}_2\text{O})_{26}$ is too small to properly describe the MHP location on the ice surface: during the optimization, the molecule was forming the additional bonds with the fixed boundary atoms, which resulted in a serious error for the energies. Therefore, the minimal clusters used in the further modeling were $(\text{H}_2\text{O})_{48}$ for (0001) surface and $(\text{H}_2\text{O})_{56}$ - for $(10\bar{1}0)$ and $(11\bar{2}0)$ planes. These clusters possess all necessary features of the ice *Ih* surface fragments. Their central part presents different sites of the real surface: dangling O and H sites as well as the different combinations of the neighboring O and H sites including the alternating rows of H and O groups as it is believed to be present in the Fletcher phase of the ice surface.^{19,20} The geometries of the clusters $(\text{H}_2\text{O})_{48}$, $(\text{H}_2\text{O})_{56}^{(1)}$, and $(\text{H}_2\text{O})_{56}^{(2)}$

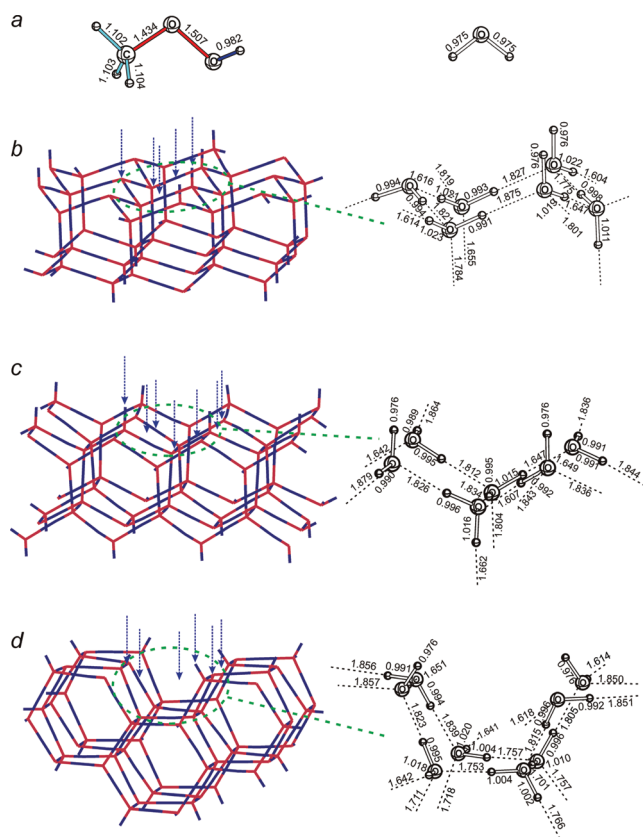


Figure 2. BLYP/6-31+G(d,p)-optimized structures of the source molecules and clusters modeling the ice Ih surface: (a) – free MHP and water molecules, (b) – $(\text{H}_2\text{O})_{48}$ modeling the (0001) plane, (c) – $(\text{H}_2\text{O})_{56}$ modeling the $(10\bar{1}0)$ plane, (d) – $(\text{H}_2\text{O})_{56}$ modeling the $(11\bar{2}0)$ plane. Dashed arrows mark the sites probed by MHP molecule to find the most favorable adsorption complexes.

optimized at the BLYP/6-31+G(d,p) level are shown in Figure 2 along with the free water and MHP molecules.

The proton ordering in the ice model deserves a special discussion. The ice crystal has the random disordering of the H sublattice, which results in exponential growth of the feasible structures when the size of the cluster increases. All of the structures have different adsorption ability and different contribution into the average adsorption energy of the bulk ice. Recently, we estimated the differences in the adsorption ability of the clusters with various proton ordering modeling the H_2O_2 adsorption on a variety of different (random) proton-disordered structures of $(\text{H}_2\text{O})_{11}$ composition.²¹ The results obtained at the B3LYP/6-31++(d,p) level showed that the effect of different proton ordering on the H_2O_2 adsorption energy is not very pronounced although it is noticeable. The differences in the adsorption energy are about 10–15% of the maximum value, which is comparable or lower than the uncertainty of the quantum chemical method or the cluster approximation itself. Therefore, in this work we used the simplified model with the proton ordering proposed earlier – P-ordered ice model of Pisani.^{22,23} This model is simple for construction and calculation, provides the proper physical parameters both for slabs and clusters (e.g., dipole moment of the bulk ice is close to zero) and it was already successfully used previously in adsorption studies.²⁴ Because the changes in the surface proton ordering result in 10–15% of adsorption energy,²¹ we

consider this value as an intrinsic uncertainty of the model used here.

The quantum chemical method used throughout the studies of the minimal clusters $(\text{H}_2\text{O})_{48}$ and $(\text{H}_2\text{O})_{56}$ was the density functional theory at the BLYP/6-31++G(d,p) level. For the whole cluster series including the larger structures, we used the PM3 method to investigate the agreement between the results obtained for small clusters with the larger models. Because of difficulties in combining the different empirical potentials developed for the pure water (TIPnP, SPC, etc.) with the potentials developed for the organic crystal packing,²⁵ we did not apply the force field approach. Instead, we used the pure electronic structure methods for the extended models although at the semiempirical level. One should notice that the PM3 method gives good agreement with the DFT calculations including the B3LYP/6-31++G(d,p) calculations as it was demonstrated in our recent study by comparison of DFT and PM3 calculated energies of 25 proton disordered structures (which were the most favorable ones from a whole set of 789 structures) of cluster $(\text{H}_2\text{O})_{11}$.²¹ Another semiempirical method AM1 was also tested in the current work. However, the geometry optimization gives a strong deformation of the equilibrium cluster structure. Because of the fact that it is assumed that the water ice has a well-defined structure at temperatures below 180 K,^{2,26} the AM1 method was rejected.

The BLYP/6-31++G(d,p) level of theory was used in all the geometry optimizations for the complexes $(\text{H}_2\text{O})_{48}$, $(\text{H}_2\text{O})_{56}$ and for some structures of $(\text{H}_2\text{O})_{72}$. The validity of this theory level was additionally tested by the geometry optimization in the extended basis set (BLYP/6-311++G(2d,2p)) performed for the $\text{MHP} \cdot (\text{H}_2\text{O})_{48}$ adsorption complex on the (0001) plane. As it will be shown below, both basis sets give comparable results. For larger clusters, however, the BLYP/6-31++G(d,p) level was impractical, and the special coarser density grid (corresponding to the Gaussian03 command “*blp/6-31++G(d,p)/auto denfit int=(grid=sg1)*”) was used for the complexes with $(\text{H}_2\text{O})_{72}$. This theory level was also used in the frequency calculations.

On the basis of the calculated frequencies, several important thermodynamic quantities can be estimated. Here, we calculated the zero-temperature enthalpy of adsorption as a sum of adsorption and zero-point energies. During the thermodynamic calculations, the contributions from the fixed boundary atoms (negative and very low frequencies) were eliminated in such a manner to keep the correct relationship between the vibrational mode numbers in the source cluster, adsorbed molecule, and adsorption complex ($N_{\text{ice}} + N_{\text{MHP}} + 6 = N_{\text{complex}}$). Because the low frequency modes give the low contributions to the enthalpy, it is believed that the elimination of these frequencies has only a small effect on the enthalpy.

Instead of probing only several adsorption sites on the surface proposed on the basis of chemical intuition or random selection, we tried to perform the most comprehensive exploration of as many as possible adsorption sites feasible on different surface planes of the ice crystal and the defects formed due to the intrusion of MHP into the ice crystal. To do that, a special computer code was used to explore the most promising starting points for the DFT optimization. The program was placing the MHP molecule in the different sites of the cluster surface selected by means of a special plan to explore the various probable coordination sites: dangling H and O atoms, H-bond midpoints, voids between the atoms (the sites which were explored are marked in Figure 2 by dashed arrows). In each site, the molecule

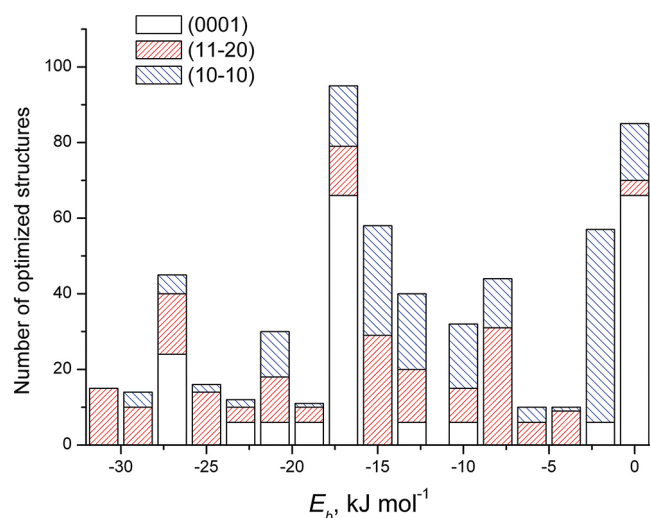


Figure 3. Distribution of the adsorption complexes of MHP at different ice crystal planes on their binding energies.

was rotated by Euler angles to cover uniformly all of the possible orientations of the molecule. For each site, we tested 20–32 different orientations additionally augmented in some cases by the different conformations (cis- and trans-) of the MHP molecule itself. It should be noted that, in all of the studied cases, the cis-conformation resulted in less stable adsorption complexes except in cases where it was rearranged during the optimization to the trans-structure. Because the number of adsorption sites studied for each cluster was typically from four to six, the complete number of the explored starting points for the optimization was 128–192 for each surface plane. Each of the constructed structures was automatically optimized then with the PM3 method and the obtained energy distribution of the optimized structures was used to select the most promising starting points for the DFT optimization.

In the same manner, we explored the intrusion of the MHP molecule into the crystalline lattice. Two different modes of incorporation were explored: intrusion into the interstitial space (cage) of the ice cluster, and the substitution of one of the H_2O molecules in a crystalline node (three different sites of the upper bilayer and two sites of the second bilayer were explored). Thus, in total about 128 different modes of the MHP intrusion were explored.

The PM3 optimization of the starting structures typically resulted in several classes of the structures distinguished by the coordination energies. The typical distribution of the preliminarily optimized structures (obtained for the $(\text{H}_2\text{O})_{48}$ cluster of (0001) surface) is shown in Figure 3. It can be seen that there is a rather significant energy difference between the most favorable and other structures. Among the most favorable structures, only one or two different kinds of structures were typically present. Therefore, only one or two most energetically favorable structures were selected from the whole set and their optimization was performed at the BLYP/6-31++G(d,p) level. In all of the clusters, all water molecules were completely free during the geometry optimization except the molecules at the side and bottom cluster borders. The border molecules were those which form fewer than 4 hydrogen bonds except the molecules at the upper plane of clusters.

All quantum chemical calculations were performed with the Gaussian03²⁷ and PC-GAMESS/Firefly^{28,29} software for the

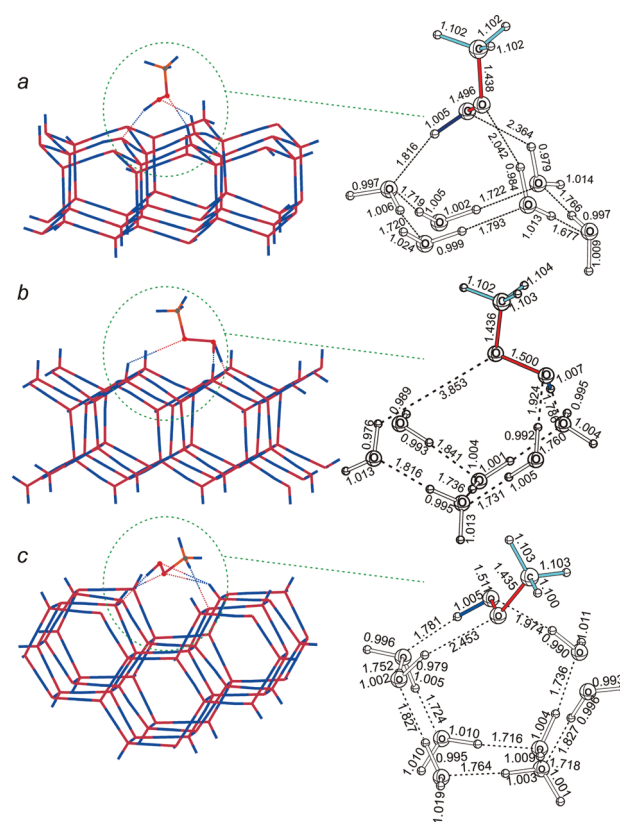


Figure 4. BLYP/6-31+G(d,p)-optimized structures of the most energetically favorable MHP adsorption complexes on the different crystal planes of ice *Ih* surface: (a) – (0001) plane, (b) – (10 $\bar{1}0$) plane, (c) – (11 $\bar{2}0$) plane.

structure optimizations on the DFT and PM3 levels. Original programs were used for the structure construction and selection. The MOLTRAN program³⁰ was applied for the output data analysis and thermodynamic calculations.

RESULTS

Adsorption on the (0001) Surface. The BLYP/6-31++G(d,p)-optimized structure of the MHP adsorption complex on the (0001) surface of the ice *Ih* is shown in part a of Figure 4. The energy of adsorption (BSSE-corrected) is $-45.3 \text{ kJ mol}^{-1}$ (Table 1). The additional optimization at the better theoretical level (BLYP/311++G(2d,2p)) results in quite similar geometry with only a slightly lower energy value of $-39.8 \text{ kJ mol}^{-1}$.

The conformation of the adsorption complex is quite similar to the structure obtained in the preliminary PM3 optimization. Another favorable conformation of the adsorption complex (higher in energy by 1.2 kJ mol^{-1}) selected on the basis of the PM3 optimization was not reproduced in the DFT calculation. During the optimization of this structure, it was rearranged to the structure similar to the most favorable one.

To test the validity of the adsorption energy value obtained with the $(\text{H}_2\text{O})_{48}$ cluster, we repeated the PM3 optimization of the most stable structure found in the preliminary search using the extending cluster series $(\text{H}_2\text{O})_{48}$, $(\text{H}_2\text{O})_{192}$, $(\text{H}_2\text{O})_{216}$ (Figure 1). The first one was the same cluster as in DFT optimization, the second one represented the slab extended in the horizontal plane, and the last one was the cluster extended both in depth and side

Table 1. BLYP/6-31++G(d,p) and BLYP/6-311++G(2d,2p) (in Square Brackets) Optimized Adsorption Energies of the MHP Molecule on the Ice Clusters

cluster/plane	cluster energy au	complex energy, ^a au	ΔE , kJ mol ⁻¹	$\Delta E + \text{BSSE}$, kJ mol ⁻¹	$\Delta H(0)$, kJ mol ⁻¹
Surface Adsorption					
(H ₂ O) ₄₈ (0001)	-3668.7669462 [-3670.0445655]	-3859.6139963 [-3860.9482416]	-51.7 [-44.8]	-45.3 [-39.8]	-35.9
(H ₂ O) ₅₆ (10 $\bar{1}$ 0)	-4280.2063157	-4471.0564797	-59.9	-53.7	-46.8
(H ₂ O) ₅₆ (11 $\bar{2}$ 0)	-4280.2488698	-4471.0958620	-51.5	-44.1	-36.2
Upper Bilayer H ₂ O Substitution at Dangling H Site					
(H ₂ O) ₄₈ (0001)	-3668.7680180	-3783.1760263	8.2 (-87.0) ^b		4.1 (-73.6)
Upper Bilayer H ₂ O Substitution at Dangling O Site					
(H ₂ O) ₄₈ (0001)	-3668.7680180	-3783.1688177	27.1 (-83.3)		18.5 (-68.0)
Interstitial Intrusion between 1st and 2nd Bilayers					
(H ₂ O) ₇₂ (0001)	-5503.2363755	-5694.0475545	42.5 ^c		
(H ₂ O) ₇₂ (0001)	-5503.2445375 ^c	-5694.0509040 ^d	56.9 ^d		
Second Bilayer H ₂ O Substitution					
(H ₂ O) ₇₂ (0001)	-5503.2445375 ^c	-5617.6212183 ^d	91.8 ^d		
(H ₂ O) ₇₂ (0001)	-5503.2339416 ^c	-5617.6095555 ^d	94.6 (-40.5) ^d		

^a Energies of H₂O and MHP molecules at the same theory level are -76.4162296 and -190.8273565 au, respectively. ^b The values in parentheses are the energies of the complex formation between MHP and the optimized cluster (H₂O)_{n-1} (the cluster without the water molecule being replaced by MHP). ^c The structure with distorted upper layer and MHP molecule shifted to the upper bilayer position. ^d The values obtained within a nonstandard DFT grid mode (*blyp/6-31++G(d,p)/auto denfit int=(grid=sg1)*). The corresponding H₂O and MHP energies are -76.4163856 and -190.8280359 au, respectively.

Table 2. PM3 Optimized Enthalpies (kJ mol⁻¹) of the MHP Coordination on the Ice Clusters of Extending Size

model	cluster size <i>n, m, l</i>	small cluster (H ₂ O) _n	medium cluster (H ₂ O) _m	large cluster (H ₂ O) _l
adsorption on (0001)	48, 192, 216	-26.3	-25.9	-26.2
adsorption on (10 $\bar{1}$ 0)	56, 108, 216	-27.5	-25.8	-27.3
adsorption on (11 $\bar{2}$ 0)	56	-30.6		
upper layer substitution at dangling H site	48, 72, 216	2.3 (-51.3) ^a	10.2	8.4
upper layer substitution at dangling O site	48, 72, 216	40.2 (-20.8)	39.3 (-29.6)	41.5 (-25.7)
interstitial intrusion	48, 72, 216	45.1	29.7	31.6
second layer substitution	48, 72, 216		46.1 (-37.0)	41.6 (-39.5)

^a The values in parentheses are the energies of the complex formation between MHP and the optimized cluster (H₂O)_{n-1} (the cluster without the water molecule being replaced by MHP).

directions. The energy of adsorption is given in Table 2. As one can see from the table, the extension of clusters results in only small changes in adsorption energy.

Adsorption on the (10 $\bar{1}$ 0) Surface. Adsorption on the (10 $\bar{1}$ 0) surface is the coordination in the valleys between parallel ridges formed by (H₂O)₆ fragments. The energy of adsorption is determined by the terminal groups located on the tops of the opposite ridges. The distribution of these groups are dependent on the proton disordering in the crystal ice. Thus, in this work it is determined by the Pisani's P-ice model. For this model, the dangling H and O atoms form the alternate rows on the tops of ridges. This is similar to the (0001) surface ordering and also in agreement with the idea of the Fletcher phase.^{19,20} For such a structure (part b of Figure 3), the DFT-optimized coordination energy (BSSE-corrected) of the most stable conformation of MHP·(H₂O)₅₆ complex is -53.7 kJ mol⁻¹. This value is remarkably higher than the corresponding coordination energy on the basal plane (-45.3 kJ mol⁻¹). As in the case of (0001) surface, the calculations of the extended clusters (H₂O)₅₆, (H₂O)₁₀₈, and (H₂O)₂₁₆ show that the results are quite stable

relative to the extension of the cluster size. During the cluster size variation, the energy changes are less than 3 kJ mol⁻¹ (Table 2).

Adsorption on the (11 $\bar{2}$ 0) Surface. Results of the preliminary exploration of the adsorption structures show that two significantly different modes of adsorption are feasible on the (11 $\bar{2}$ 0) surface. The first one is the position between two walls formed by six water molecules and the second one — on the top of wall. The PM3 energy of adsorption on the wall is significantly lower than at the position between the walls (about 31 and 20 kJ mol⁻¹). The BSSE-corrected DFT adsorption energy (-44.1 kJ mol⁻¹) of the optimized most stable conformation of the adsorption complex on the (H₂O)₅₆ cluster (part c of Figure 4) is quite close to the energy of adsorption on the (0001) surface.

Incorporation of MHP into the Surface Layer of the Water Ice Crystal with Substitution of One H₂O Molecule. The incorporation of MHP into the upper layer of the ice crystal with substitution of one H₂O molecule is dependent on the kind of the crystalline node replaced. The substitution at the (0001) surface is possible at the dangling H (referred hereafter dH) or dangling O (dO) sites. Then, the energy of substitution will be

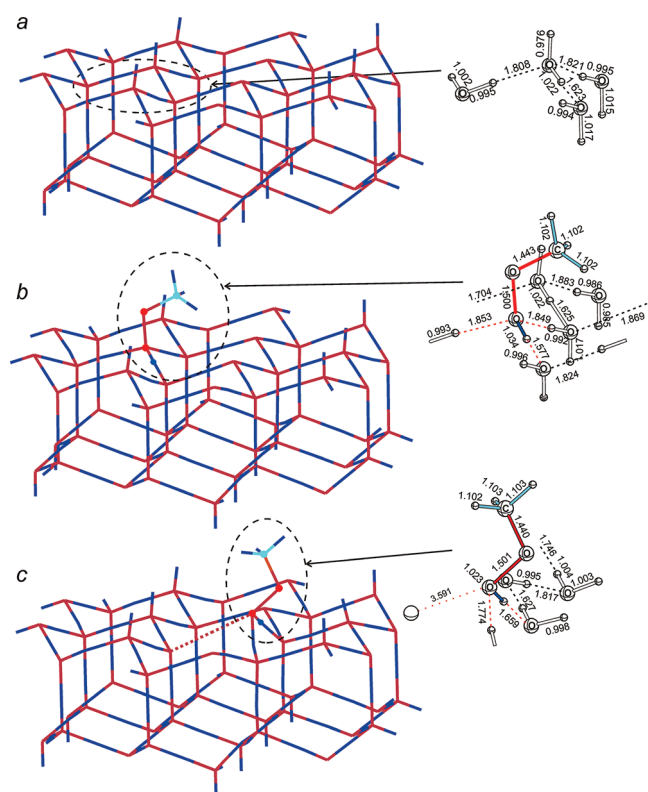


Figure 5. BLYP/6-31++G(d,p)-optimized structures of the MHP incorporated into the surface layer of the (0001) crystal plane of ice Ih: (a) – source cluster (H_2O)₄₈, (b) – MHP incorporated at the dangling H site, (c) – MHP incorporated at the dangling O site.

dependent on whether the OCH_3 group is dangling outside or built-in into the surface (with coordination of a second oxygen atom). During the preliminary exploration performed with the (H_2O)₇₂ cluster, the most favorable coordination site was always dH with dangling OCH_3 fragments. The structures shown in Figure 5 demonstrate the most favorable structures optimized at the BLYP/6-31++G(d,p) level. The energies relatively to the uncoordinated species are positive at both DFT and PM3 levels for the clusters of any considered size. For the structure shown in part b of Figure 5 (substitution at the dangling H site) it gives 8.7 kJ mol^{-1} , for site part c of Figure 5 (substitution at the dangling O site) it yields 27.1 kJ mol^{-1} . It is interesting that the corresponding energies of incorporation calculated for the relaxed defective clusters, that is the optimized clusters with one H_2O molecule removed from the site of MHP incorporation, were highly negative (see the values of Table 1 given in parentheses).

Intrusion of MHP into the Interstitial Cage. Intrusion of MHP was modeled with the cluster (H_2O)₇₂ for all of the intrusion modes because this is the minimal structure having two bilayers of unfixed water molecules inside the cluster. This also provides the proper structure for the interstitial intrusion if the MHP molecule is placed into the cage between two upper bilayers. To reduce the computation time, the regular DFT calculations were augmented with the calculations using the coarser density grid as described in the section Surface models and theoretical methods. Both of these different modes resulted in similar geometry parameters and incorporation energies.

It was found that the location of MHP molecules in the interstitial cage results in a significant increase in energy relative

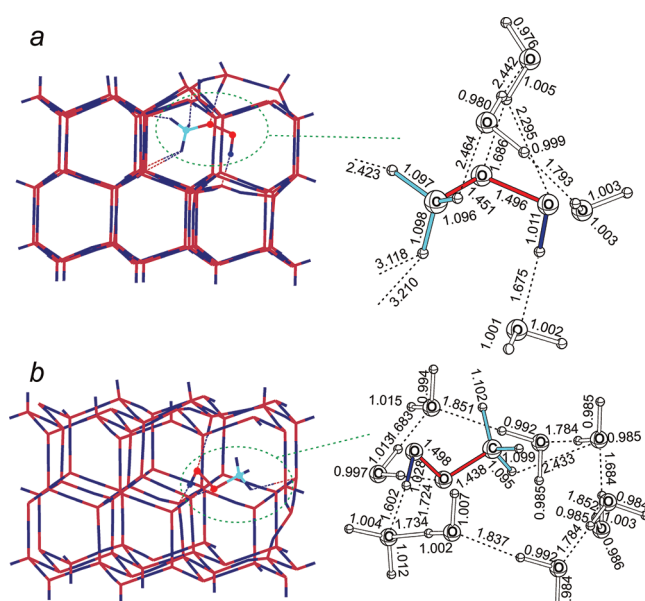


Figure 6. Optimized structures of the MHP incorporated into the ice Ih crystal: (a) – interstitial intrusion, (b) – substitution of second layer node.

to the free cluster. Although there are several possible stable structures, all of them are unfavorable from the energetic point of view in comparison with the surface adsorption. The most stable conformation is characterized by the 42.5 kJ mol^{-1} increase of energy relatively to the free molecule and cluster (Table 1). The optimized structure is shown in part a of Figure 6. At the PM3 level, the corresponding energy values are also positive although remarkably lower (about 30 kJ mol^{-1}). Extending of the cluster model results in only slight changes: from 29.7 for (H_2O)₇₂ to 31.6 kJ mol^{-1} for the (H_2O)₂₁₆ cluster. In some optimized structures, the MHP molecule was pushed out to the surface breaking up the upper layer. However, even if the cluster structure was kept intact the energy was quite unfavorable for the interstitial incorporation.

Incorporation of MHP into the Deeper Layers of the Water Ice Crystal with Substitution of One H_2O Molecule. The incorporation of MHP into the second and deeper layers of the ice crystal cannot be modeled with the minimal clusters (H_2O)₄₈ or (H_2O)₅₆ because atoms of the second layer are fixed in crystalline positions. The energy of such kind of incorporation was estimated using the cluster (H_2O)₇₂. The DFT calculations were carried out using the coarser density grid. For all of the optimized models, the substitution of the second layer H_2O molecule with MHP was quite unfavorable. The estimated energies of incorporation were higher with about 90 kJ mol^{-1} (Table 1), and the most stable structure is shown in part b of Figure 6. The corresponding PM3 values are also positive although significantly lower (46 kJ mol^{-1}). The influence of the cluster extension is only minor (Table 2).

Vibrational Frequencies. Frequency calculations carried out for (H_2O)₄₈ and (H_2O)₅₆ clusters with the MHP molecules adsorbed on different crystal planes demonstrate that there should be no new intense bands or remarkable band shifts in the spectral range between 1000 and 3600 cm^{-1} . All of the new bands due to the MHP adsorption are masked by the broad bands of ice. However, the calculations show that the low-frequency wing of

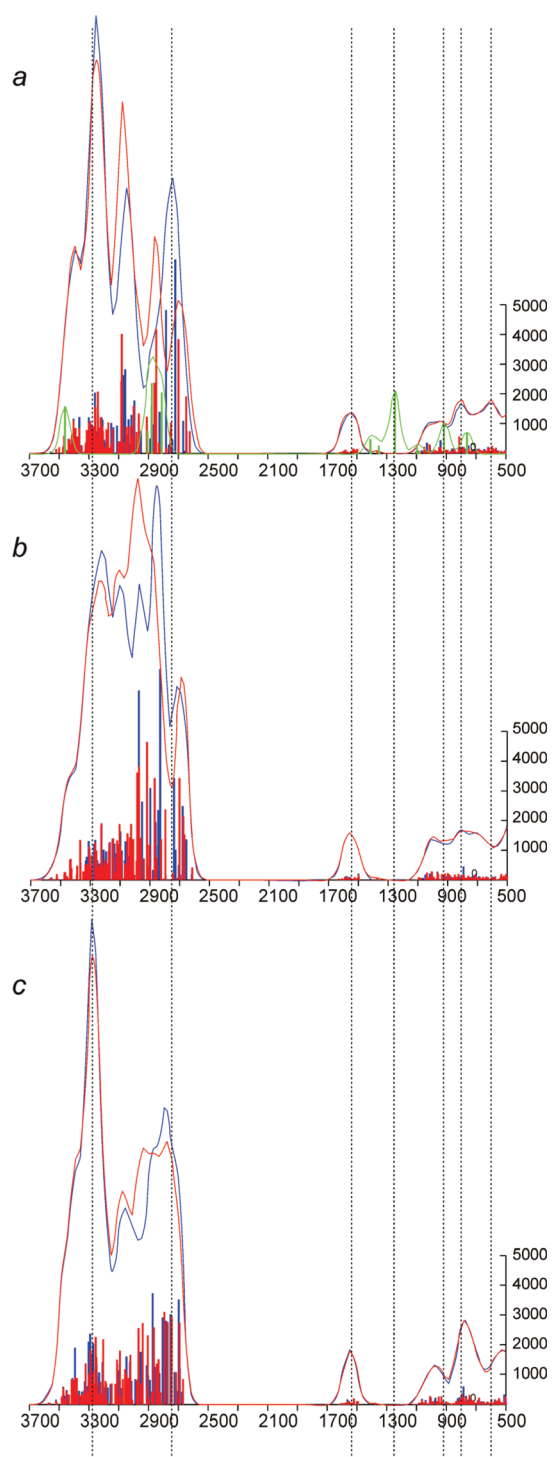


Figure 7. BLYP/6-31++G(d,p) calculated IR spectra of ice *Ih* clusters (blue trace), MHP (intensity magnified by 50 times, green trace), and the clusters with adsorbed MHP (red trace): (a) – $(\text{H}_2\text{O})_{48}/(0001)$ plane, (b) – $(\text{H}_2\text{O})_{56}/(10\bar{1}0)$ plane, (c) – $(\text{H}_2\text{O})_{56}/(11\bar{2}0)$ plane. Horizontal axis – calculated frequencies in cm^{-1} scaled by factor 0.957, vertical axis – calculated intensities in km/mol .

the ice band in the region $2700\text{--}2900\text{ cm}^{-1}$ can undergo rather significant reshaping (accompanied with simultaneous growth of intensity near 3100 cm^{-1}) due to the MHP adsorption on the (0001) plane (part a of Figure 7). At the same time, adsorption

on the $(10\bar{1}0)$ plane should result in significant reshaping of the ice band (increasing intensity) around 3000 cm^{-1} (part b of Figure 7). If this reshaping would be observed in the experiment, it could serve as a measure of adsorption on different planes of the ice crystal. The $(11\bar{2}0)$ adsorption gives no remarkable changes in IR spectra (part c of Figure 7).

DISCUSSION

The data of Table 2 show that the minimal clusters $(\text{H}_2\text{O})_{48}$ and $(\text{H}_2\text{O})_{56}$ are already large enough to sufficiently describe the crystal environment effects for the adsorption modes. However, they are not suitable for the modeling of the intrusion and the second layer substitution modes. For such purposes, the cluster $(\text{H}_2\text{O})_{72}$ seems to be a good model although probably not the minimal one.

On the basis of the data from Tables 1 and 2, we can establish the energetic series of the MHP interaction with the crystalline ice particles (from the most to the less favorable structures):

$$\begin{aligned} &(\text{surface adsorption}) < (\text{upper layer dH substitution}) \\ &< < (\text{upper layer dO substitution}) < (\text{interstitial intrusion}) \\ &\leq (\text{second layer incorporation}) \end{aligned}$$

Comparison with the available experimental data and theoretical estimates of other authors shows that the adsorption energy of the free MHP molecules on different surfaces is close to the typical enthalpies of the ice *Ih* sublimation:³¹ $\Delta_{\text{subl}}H$ ranges from 47 ($T = 0\text{ K}$) to 56 kJ mol^{-1} ($T = 273\text{ K}$). At the same time, the energy of MHP incorporated into the ice crystal (both in interstitial and node positions) is remarkably higher than the energy of MHP in liquid water.^{8–10} In particular, the positive values of 42–57 kJ mol^{-1} obtained here for the interstitial intrusion is in sharp contrast with the $\Delta_{\text{sol}}H^0(298)$ value for the MHP solution in water (-43.6 kJ mol^{-1}) measured by O’Sullivan et al.⁸ (It should be noted that in ref 8 $\Delta_{\text{sol}}H^0(298)$ is given as $+43.6\text{ kJ mol}^{-1}$, however, the graphical dependence of the Henry’s law constant on $1/T$ shows that the value should be negative). It can be explained by the fact that the solute environment in liquid water is quite different from the crystalline structure. Thus, the incorporation of MHP into the ice crystal at higher temperatures should result in a significant reconstruction of the closest environment that could be observed in the MD or MC studies. This also corresponds to the results of recent quantum chemical studies of acetone incorporation into the ice crystal^{25,32} where the positive energies were obtained even for the substitution of several water molecules.

At the BLYP level, the most favorable adsorption complexes are formed at the $(10\bar{1}0)$ plane. The MHP molecule at this coordination mode forms two virtually equal H-bonds between the OOH group and the neighboring dangling OH and dangling O surface groups. These two groups are located close to each other and allow the formation of two H-bonds equal in bond lengths and energies. In other cases, the H-bonds $\text{O}\cdots\text{H}-\text{O}(\text{OMe})\cdots\text{H}$ formed between the OOH group and the surface H and O atoms are not equal in length: $\text{O}(\text{OMe})\cdots\text{H}$ is remarkably longer. This probably results in a remarkable decrease of adsorption energy. The calculations show that the formation of the H-bonded adsorption complexes with dangling H-atom of MHP ($\text{H}\cdots\text{O}(\text{H})\text{O}(\text{Me})\cdots\text{H}$) is quite unfavorable.

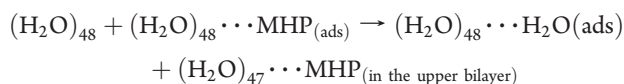
It is interesting to consider the structures of adsorption complexes and the cause of stronger binding in the case of $(10\bar{1}0)$ adsorption. Earlier,^{33,34} it was demonstrated that the energy of

adsorption complexes of ethanol at the ice (0001) surface correlates well with the numbers of short and long hydrogen bonds formed between admolecule and surface. However, the structures shown in Figure 4 have the same numbers of H-bonds (two short ones and single long one) and cannot be discriminated in such a simple manner. More generally, we can consider the $O \cdots H$ contact as an H-bond when the $O \cdots H$ distance is less than the preset threshold r_{\max} . If r_{\max} is chosen as 2.0 Å, the numbers of H-bonds N_{HB} formed at (0001), (10 $\bar{1}$ 0), and (11 $\bar{2}$ 0) surfaces equals to 1, 2, 2, respectively. Similarly, if $r_{\max} = 2.5$ Å then $N_{\text{HB}} = 3, 2, 3$, and if $r_{\max} = 3.0$ Å, then $N_{\text{HB}} = 3, 3, 6$. These values poorly correlate with the data of Table 1. Thus, there is no significant correlation between N_{HB} and the DFT calculated adsorption energies on the basis of the simple H-bonds count. The good correlation between the binding energy and the adsorption complex structure was found for the empirical expression involving the H-bond lengths:

$$E_b = a \left(\sum_{i=1}^3 r_i^{-n} \right) + b$$

Here r_i are three H-bond lengths $r(O \cdots H)$ between the MHP and water molecules shown in Figure 4, $E_b = -(\Delta E + \text{BSSE}) - \text{the BSSE corrected binding energy calculated by DFT (Table 1)}$; a, b – regression coefficients. Among all of the integer values of n between -12 and 12 , the best correlation ($R^2 = 0.9984$) takes place for $n = 1$: $a = -69.227$, $b = 146.43$. This gives $E_b = 45.1, 53.7, 44.3 \text{ kJ mol}^{-1}$ respectively for the structures shown in Figure 4, in excellent agreement with the DFT calculated values. However, the negative a and positive b proposes that the main effect discriminating each $O \cdots H$ pair in this model is the interatomic Coulomb repulsion with approximately equal attraction of the adsorption complexes as a whole. From this point of view, the stronger coordination between MHP and ice at the (10 $\bar{1}$ 0) surface takes place due to the possibility to form the long $O \cdots H$ contact (3.853 Å) with two short and strong $O \cdots H$ bonds.

The energy of substitution of the water molecules in the upper surface layer by the adsorbed MHP molecule is positive. On the basis of the data from Table 1 and the energy of the H_2O adsorption on $(\text{H}_2\text{O})_{48}$ (0001) (simple optimization without extensive search of the most favorable structure gives $-46.3 \text{ kJ mol}^{-1}$), the lowest energy of the process



is estimated to be 13.6 kJ mol^{-1} . We conclude that the interaction of the MHP molecules with ice particles in the middle atmosphere is completely restricted by the surface adsorption without any remarkable diffusion of MHP into the ice crystal body. Any remarkable enrichment of the ice particles by MHP can take place only at the special atmospheric condition of fast ice particle growth when the adsorbed MHP molecules are buried by the new layers of the condensed water.

Because the MHP molecule is located at the ice surface or incorporated into the upper layers of the ice crystal under conditions of the middle atmosphere, the MHP coordinated on the ice particles is open for the direct reactions with other reactive species that attack the ice surface from the gas phase. It also means that the coordinated MHP molecule is available for direct photolysis, that is primary photochemical reactions should

be initiated already with source photons and not from the photons dissipated by the crystal lattice.

In contrast with the coordination in the unconstrained clusters,¹⁵ the most favorable MHP incorporation complex (MHP at dH site, part b of Figure 5) is coordinated with a dangling OCH_3 fragment with only a small participation of the second O atom in the hydrogen bonds. The remarkable participation of the second oxygen in the MHP–surface coordination takes place only at the dO site (part c of Figure 5), which is significantly higher in energy. Although authors of ref 15 did not report separately the MHP–cluster binding energy, their average value of 29.0 kJ mol^{-1} (calculated from $-41.52 \text{ kcal mol}^{-1}$ of reported total BSSE-corrected interaction energy for $\text{MHP} \cdot (\text{H}_2\text{O})_5$ at dH site) is remarkably lower than the results obtained in the current work for the larger ice-like clusters ($40\text{--}50 \text{ kJ mol}^{-1}$). Probably, this fact reflects the differences between the clusters with coordinated oxygen of $-\text{OCH}_3$ (in Kulkarni's clusters) and additionally coordinated HO– fragment (MHP with dangling $-\text{OCH}_3$). It follows from our results that the coordination ability of HO–oxygen is higher than that for $-\text{OCH}_3$ oxygen, and this results in higher binding energy.

It should be mentioned that one can consider the energetic effects of intrusion into the upper and second layers either as the substitution of H_2O by MHP molecule or as the MHP complex formation on defective clusters with H_2O vacancies (values in Table 2 shown in parentheses). In the second case, this process is highly exothermic and probably characterizes the conditions of the fast nonequilibrium co-condensation. Such a model is rarely used for the conditions of upper atmospheric layers. Thus, it is believed that more reliable estimates are those shown in Table 2 without parentheses. Independently on the method of the binding energy estimation, the data show that the incorporation into the surface layer at the dO site is much less preferable than the similar process at the dH site.

CONCLUSIONS

The adsorption of the MHP molecule on different sites of the hexagonal water ice crystal has been studied using the H_2O clusters of various size and structure. The results obtained allow drawing the following conclusions:

- 1 The maximum binding energy of the MHP adsorption on the ice-like clusters is about 54 kJ mol^{-1} with typical values on the order of $40\text{--}54 \text{ kJ mol}^{-1}$ depending on the site and surface plane. The adsorption on different planes results in remarkable differences in the binding energy: $55\text{--}60 \text{ kJ mol}^{-1}$ for the (10 $\bar{1}$ 0) plane and $40\text{--}45 \text{ kJ mol}^{-1}$ – for the (0001) and (11 $\bar{2}$ 0) planes. The best estimate of the binding energy for the adsorption on the (0001) plane is 39.8 kJ mol^{-1} (BLYP/6-311++G(2d,2p)).
- 2 The zero-temperature adsorption enthalpies range from -36 kJ mol^{-1} (adsorption on (0001) and (11 $\bar{2}$ 0) surfaces) to -47 kJ mol^{-1} (on the (10 $\bar{1}$ 0) plane). These values are close to the experimental values of zero-temperature sublimation enthalpy of ice Ih (47 kJ mol^{-1})³¹ and the enthalpy of solution of MHP in water ($-43.6 \text{ kJ mol}^{-1}$).⁸ Upper bilayer H_2O substitutions are characterized by positive $\Delta H(0)$ values with 4.1 kJ mol^{-1} (at dangling H sites) and 18.5 kJ mol^{-1} (at dangling O sites).
- 3 The interstitial intrusion is less favorable (ΔE ranges from 34 to 43 kJ mol^{-1}) than the upper layer substitution (8 to 27 kJ mol^{-1}) but much more favorable than the

substitution of the H₂O molecules in the internal bilayers (91 kJ mol⁻¹).

- 4 The good convergence of results obtained for the clusters (H₂O)₄₈ and (H₂O)₅₆ with those obtained for the larger models shows that DFT within the cluster approximation is a model good enough to be used on its own without any corrections for the environmental effects of the remaining part of the ice crystal. These clusters permit already a good presentation of the different coordination modes and demonstrate quite good agreement in comparison with the extended models. Extension of the models with clusters containing up to 216 water molecules does not result in significant changes of the coordination energy.

ASSOCIATED CONTENT

S Supporting Information. Cartesian coordinates for the DFT-optimized structures in Figures 2 and 4–6. This material is available free of charge via the Internet at <http://pubs.acs.org>.

AUTHOR INFORMATION

Corresponding Author

*E-mail: ignatov@ichem.unn.ru.

ACKNOWLEDGMENT

This work was partially supported by the Russian foundation for Basic Research (projects No. 11-03-00085, 09-03-00706a, and 10-05-01112). S.K.I. and M.Y.K. thank the German Academic Exchange Service (DAAD) and the Alfred Wegener Institute for Polar- and Marine Research, Bremerhaven for fellowship supports. A.I.P. is thankful to SFU Super-computer Centre for generous donation of CPU-time.

REFERENCES

- (1) Wayne, R. P. *Chemistry of Atmospheres*; Clarendon Press: Oxford, 1991.
- (2) Girardet, C.; Toubin, C. *Surf. Sci. Rep.* **2001**, *44*, 159.
- (3) Sennikov, P. G.; Ignatov, S. K.; Schrems, O. *ChemPhysChem* **2005**, *6*, 392.
- (4) Frey, M. M.; Hutterli, M. A.; Chen, G.; Sjostedt, S. J.; Burkhart, J. F.; Friel, D. K.; Bales, R. C. *Atmos. Chem. Phys.* **2009**, *9*, 3261.
- (5) Riedel, K.; Weller, R.; Schrems, O.; König-Langlo, G. *Atmos. Environ.* **2000**, *34*, 5225.
- (6) Ignatov, S. K.; Sennikov, P. G.; Jacobi, H.-W.; Razuvaev, A. G.; Schrems, O. *Phys. Chem. Chem. Phys.* **2003**, *5*, 496.
- (7) Kamboures, M. A.; Nizkorodov, S. A.; Gerber, R. B. *Proc. Natl. Acad. Sci. U.S.A.* **2010**, *107*, 6600.
- (8) O'Sullivan, D. W.; Lee, M.; Noone, B. C.; Heikes, B. G. *J. Phys. Chem.* **1996**, *100*, 3241.
- (9) Lind, J. A.; Kok, G. L. *J. Geophys. Res., [Atmos.]* **1986**, *91*, 7889.
- (10) Lind, J. A.; Kok, G. L. *J. Geophys. Res., [Atmos.]* **1994**, *99*, 21119.
- (11) Alkorta, I.; Elguero, J. *J. Chem. Phys.* **2002**, *117*, 6463.
- (12) Du, D.; Fu, A.; Zhou, Z. *Chem. Phys. Lett.* **2004**, *392*, 162.
- (13) Kulkarni, A. D.; Rai, D.; Bartolotti, L. J.; Pathak, R. K. *J. Mol. Struct.: Theochem.* **2007**, *824*, 32.
- (14) Du, D.; Zhou, Z. *Int. J. Quantum Chem.* **2005**, *106*, 935.
- (15) Kulkarni, A. D.; Rai, D.; Bartolotti, L. J.; Pathak, R. K. *J. Chem. Phys.* **2009**, *131*, 4310.
- (16) Fry, J. L.; Matthews, J.; Lane, J. R.; Roehl, C. M.; Sinha, A.; Kjaergaard, H. G.; Wennberg, P. O. *J. Phys. Chem. A* **2006**, *110*, 7072.
- (17) Bach, R. D.; Su, M.-D.; Schlegel, H. B. *J. Am. Chem. Soc.* **1994**, *116*, 5379.
- (18) Urakawa, A.; Bürgi, T.; Skrabal, P.; Bangerter, F.; Baiker, A. *J. Phys. Chem. B* **2005**, *109*, 2212.
- (19) Buch, V.; Groenzin, H.; Li, I.; Shultz, M. J.; Tosatti, E. *Proc. Natl. Acad. Sci. U.S.A.* **2008**, *105*, 5669.
- (20) Fletcher, N. H. *Philos. Mag. B* **1992**, *66*, 109.
- (21) Ignatov, S. K.; Razuvaev, A. G.; Sennikov, P. G.; Schrems, O. *J. Mol. Struct.: Theochem.* **2009**, *908*, 47.
- (22) Pisani, C.; Casassa, S.; Ugliengo, P. *Chem. Phys. Lett.* **1996**, *253*, 201.
- (23) Casassa, S.; Ugliengo, P.; Pisani, C. *J. Phys. Chem.* **1997**, *106*, 8030.
- (24) Marinelli, F.; Allouche, A. *Chem. Phys.* **2001**, *272*, 137.
- (25) Hammer, S. M.; Panisch, R.; Kobus, M.; Glinnemann, J.; Schmidt, M. U. *Cryst. Eng. Comm.* **2009**, *11*, 1291.
- (26) Kroes, G.-J. *Surf. Sci.* **1992**, *275*, 365.
- (27) Frisch, M. J.; Trucks, G. W.; Schlegel, H. B.; Scuseria, G. E.; Robb, M. A.; Cheeseman, J. R.; Montgomery Jr., J. A.; Vreven, T.; Kudin, K. N.; Burant, J. C.; Millam, J. M.; Iyengar, S. S.; Tomasi, J.; Barone, V.; Mennucci, B.; Cossi, M.; Scalmani, G.; Rega, N.; Petersson, G. A.; Nakatsuji, H.; Hada, M.; Ehara, M.; Toyota, K.; Fukuda, R.; Hasegawa, J.; Ishida, M.; Nakajima, T.; Honda, Y.; Kitao, O.; Nakai, H.; Klene, M.; Li, X.; Knox, J. E.; Hratchian, H. P.; Cross, J. B.; Adamo, C.; Jaramillo, J.; Gomperts, R.; Stratmann, R. E.; Yazyev, O.; Austin, A. J.; Cammi, R.; Pomelli, C.; Ochterski, J. W.; Ayala, P. Y.; Morokuma, K.; Voth, G. A.; Salvador, P.; Dannenberg, J. J.; Zakrzewski, V. G.; Dapprich, S.; Daniels, A. D.; Strain, M. C.; Farkas, O.; Malick, D. K.; Rabuck, A. D.; Raghavachari, K.; Foresman, J. B.; Ortiz, J. V.; Cui, Q.; Baboul, A. G.; Clifford, S.; Cioslowski, J.; Stefanov, B. B.; Liu, G.; Liashenko, A.; Piskorz, P.; Komaromi, I.; Martin, R. L.; Fox, D. J.; Keith, T.; Al-Laham, M. A.; Peng, C. Y.; Nanayakkara, A.; Challacombe, M.; Gill, P. M. W.; Johnson, B.; Chen, W.; Wong, M. W.; Gonzalez, C.; Pople, J. A. *Gaussian 03*, Rev. E.01; Gaussian, Inc.: Pittsburgh PA, 2007.
- (28) Schmidt, M. W.; Baldrige, K. K.; Boatz, J. A.; Elbert, S. T.; Gordon, M. S.; Jensen, J. H.; Koseki, S.; Matsunaga, N.; K.A., N.; Su, S. J.; Windus, T. L.; Dupuis, M.; Montgomery, J. A. *J. Comput. Chem.* **1993**, *14*, 1347.
- (29) Granovsky, A. A. *PC GAMESS*, Firefly version 7.1.G, <http://classic.chem.msu.su/gran/firefly/index.html>. (access date 03.24.2011)
- (30) Ignatov, S. K. *MOLTRAN*: A program for molecular visualization and thermodynamic calculations; Nizhny Novgorod: N.I. Lobachevsky State University of Nizhny Novgorod, 2009. <http://ichem.unn.ru/Moltran>. (access date 03.24.2011)
- (31) Feistel, R.; Wagner, W. *Geochim. Cosmochim. Acta* **2007**, *71*, 36.
- (32) Somnitz, H. *Phys. Chem. Chem. Phys.* **2008**, *11*, 1033.
- (33) Thierfelder, C.; Hermann, A.; Schwerdtfeger, P.; Schmidt, W. *G. Phys. Rev. B* **2006**, *74*, 045422(1).
- (34) Thierfelder, C.; Schmidt, W. *G. Phys. Rev. B* **2007**, *76*, 195426(1).